New Techniques for VFT Mitigation in GIS

M. A. Abd-Allah[1], A. Said[1], and Ebrahim A. Badran[2]
[1]Faculty of Engineering at Shoubra, Benha University, Egypt
[2]Faculty of Engineering, Mansoura University, Egypt

Abstract:
Switching operations in a Gas Insulated Substations (GIS) generate very fast transient over voltages (VFTO) which are dangerous for the transformer and the system insulation because of their short rise time. Under special circumstances the overvoltages can arise close to the transformer Basic Insulation Level (BIL). The reduction of VFTO amplitudes is considered main challenges. Therefore, VFTO in the 220 kV Wadi-Hoff GIS is analyzed and the worst case for disconnector switching is predicted using EMTP/ATP in this paper. VFTO mitigation techniques are studied in this work. Furthermore, in this paper, proposed techniques are presented for mitigating the VFTO. The proposed techniques can be used by the maintenance engineers, transformer designers, and GIS insulation manufactures. The results show that the proposed techniques highly reduce the VFTO in a simple manner.

Keywords: GIS, VFT, Mitigation Techniques, EMTP/ATP.

1. Introduction

GIS is widely used in electric power system in recent decades because of its advantages such as compact size, protection from pollution, a few maintenance, and high reliability. In spite of these advantages, GIS has unique problems, such as the very fast voltage increase due to reflections of switching transients at various junctions within the GIS [1-2]. These transients are originated within the GIS any time there is an instantaneous change in voltage. They have very short rise times, in the range of 4 to 100 ns, and are normally followed by oscillations having frequencies in the range of 100 kHz to 50 MHz [2]. They cause traveling waves internally inside the GIS, traveling from GIS bushing to external components. This can lead to damage the insulation of internal busbar and transformer, which influent the operating reliability of GIS, accelerate aging of transformer insulation and reduce transformer life [1-3]. Also, VFTO associated with Very Fast Transient Currents (VFTC) radiate electromagnetic fields during its propagation through the coaxial GIS bus section. The transient electromagnetic fields get coupled to the control equipment or data cables of the GIS [4].

In fact, the response behavior of zinc oxide (ZnO) surge arresters to such Very Fast Transients (VFT) is not well characterized, and the turn-on time of ZnO surge arresters may be much longer than the rise times of the VFT. Therefore, the traditional ZnO surge arresters cannot suppress the wave steepness because surge arresters do not act fast enough to prevent the switching transients with steep front [5].

This paper investigates the VFTO resulted from the operation of disconnector switches at different sensitive points internal and external the 220 kV Wadi-Hoff GIS. The 220 kV Wadi-Hoff GIS is taken as a case study. Therefore, VFTO in the 220 kV Wadi-Hoff GIS is analyzed and the worst case for disconnector switching is predicted using EMTP/ATP.

VFTO mitigation techniques are studied in this work. Furthermore, in this paper, proposed techniques are presented for mitigating the VFTO. The proposed techniques can be used by the maintenance engineers, transformer designers, and GIS insulation manufactures. The results show that the proposed techniques highly reduce the VFTO in a simple manner.

2. Modeling of the 220 kV Wadi-Hoff GIS

Due to the traveling nature of the transients, the different components can be modeled by distributed parameter lines, surge impedances and traveling times. Each GIS section is simulated by its equivalent capacitance and inductance, which can be determined as follows [6-7].

$$C = 2\pi\varepsilon \Big/ \ln D/d \qquad (\varepsilon \approx \varepsilon o) \qquad F/m \qquad (1)$$

$$L = \mu \ln \frac{D}{d} \Big/ 2\pi \qquad H/m \qquad (2)$$

$$Z_0 = \sqrt{L/C} = \frac{\sqrt{\varepsilon\mu}}{2\pi} \ln\frac{D}{d} \approx 60 \ln\frac{D}{d} \qquad \Omega \qquad (3)$$

$$v = \frac{1}{\sqrt{LC}} \qquad m/s \qquad (4)$$

transformers. The feeders are connected in a two busbar arrangement with a bus coupler. The equivalent circuits of the different GIS components and where C and L are the capacitance and the inductance of the GIS busbar, respectively. d is the outside diameter of the GIS busbar and D is the inner diameter of the GIS enclosure. Z0 is the surge impedance and v is the propagation velocity.

The single line diagram of the substation under study is illustrated in Fig. 1. The 220/66/11 kV Wadi-Hoff substation under study consists of four incoming feeders, two feeders each of 30 km length, and the other two feeders each of 3 km length. The substation includes three 125 MVA, 220/66/11 kV, power the values of the different parameters in the simulation are summarized in Table 1.

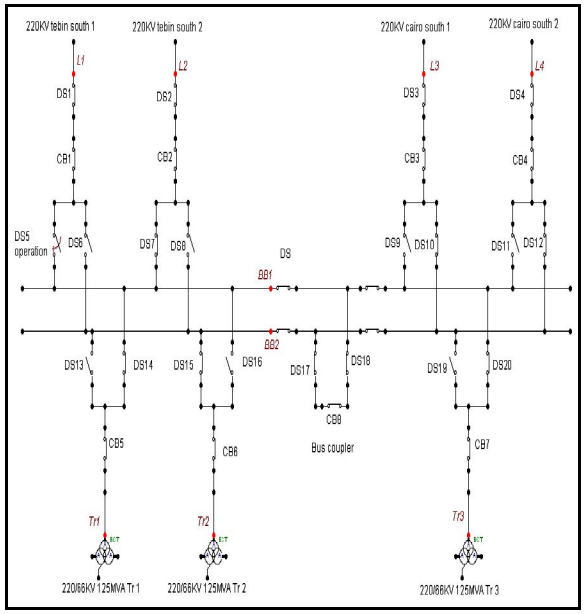

Fig. 1: Typical single line diagram for Wadi-Hoff GIS

Table.1: Information for simulation

GIS Busbar	Z_0 = 70 Ω and ν=270 m/μs
Circuit Breaker	In the closed position: impedance of 70 Ω In the open position: capacitances of 90 pF (either end to ground) and 50 pF(between contacts)
Disconnector, and Earthing Switch	In the closed position: impedance of 70 Ω In the open position: capacitances of 30 pF (either end to ground) and 30 pF(between contacts)
Potential Transformer	Capacitance of 100 pF towards ground
Current transformer	Z_0 = 70 Ω and ν=270 m/μs
Surge Arrester	200 pF in series with a grounding resistance of 0.1
Overhead Transmission Line	Z_0 = 250 Ω and ν=300 m/μs
Elbows, Spacers, and Spherical Shields	lumped capacitance of 15 pF towards ground
Bushing	Impedance of 70 Ω and 100 pF towards ground

The behavior of the spark in disconnector operations can be represented by a dynamically variable resistance with a controllable collapse time [2]. The disconnector switch (DS) restrikes are modeled as an exponentially decaying resistance in series with a small resistance. This is implemented using a Type-91, TACS time-varied resistance in EMTP/ ATP. The variable resistance is calculated from the following equation:

$$R(t) = R(0)e^{\frac{-t}{\tau}} + r \qquad (5)$$

where R(0) is 10^{12} ohm and the time constant τ is 1 ns. r represents the spark resistance after voltage breakdown and is assumed to be 0.5Ω [2, 3, 8]. During the GIS DS closing operation, the voltage breakdown takes about 4 ns, so the DS closing event is modeled as an exponentially decreasing resistance. The nonlinear resistance decreases from high value (10^{12}) to 0.5Ω in about 5 ns as shown in Fig. 2.

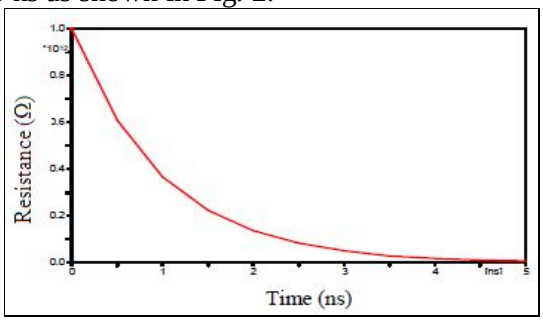

Fig. 2: DS resistance behavior during closing event

At high frequencies, the winding of transformer behaves like a capacitive network consisting of series capacitances between turns and coils, and shunt capacitances between turns and coils to the grounded core and transformer tank. So, the transformers are simulated in this work by their surge capacitances. These equivalent capacitances are in the range from 2 to 10 nF [1, 2, 3]. The transformer is modeled as a capacitor with 2 nF as given in [2]. EMTP/ATP is used to simulate the substation under study. Fig. 3 illustrates the 220 kV Wadi-Hoff GIS model in EMTP/ATP.

3. Overvoltages of Disconnector Switching

There are several switching operations to achieve some purpose such as energizing feeders, energizing transformer, CB maintenance, etc. At energizing feeders or transformer, disconnector is closed firstly, and then the CB is closed.

Table 2 shows different operating modes of disconnectors in the studied system.

At the operating modes of disconnector, the VFTO is calculated at the internal points of GIS (BB1 and BB2), the transformers terminals (Tr1, Tr2, and Tr3) and the GIS terminals such as at SF6/air bushing (L1, L2, L3, and L4). Fig. 4 shows the VFTO at several points due to different operating modes of disconnector switching. It can be seen that mode#1 is the worst case of disconnector operation in the studied substation. It is observed that the peak magnitude of the generated VFTO at Tr1is about 2.04 pu, while it is about 1.60 pu at Tr2, 1.58 pu at Tr3, 1.44 pu at L2, 1.14 pu at L3, 1.13 pu at L4, 1.22 pu at BB1 and 1.14 pu at BB2. Also, the wave shape of the generated VFTO at Tr1 is shown in Fig. 5.

4. VFTO Suppression Techniques

Up to date, the main challenges are the reduction of VFTO amplitudes. The researchers concerns on finding the optimum technique for suppressing VFTO. Several techniques are used to reduce the harmful effects of the VFTO [2, 5, 7, 8, 9]. The important techniques are studied in this work to choice the suitable technique for suppressing the VFTO value to a safe one [11].

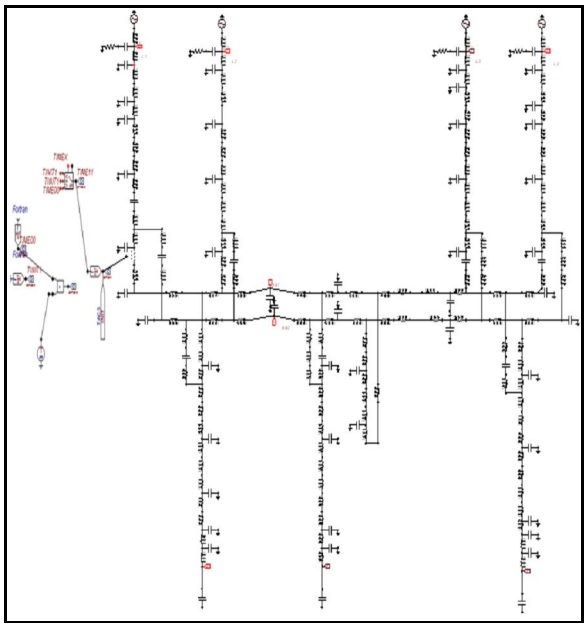

Fig. 3: EMTP/ATP Model for Wadi-Hoff GIS

Table 2: Operating modes of various disconnectors in 220 kV

Mode	Power Supply	Opened CB	Operating DS
#1	line 1 out	CB1	DS 5
#2	line 2 out	CB2	DS 7
#3	line 3 out	CB3	DS 10
#4	line 4 out	CB4	DS 12
#5	All lines connected	CB5	DS 14
#6	All lines connected	CB6	DS 15
#7	All lines connected	CB7	DS 20

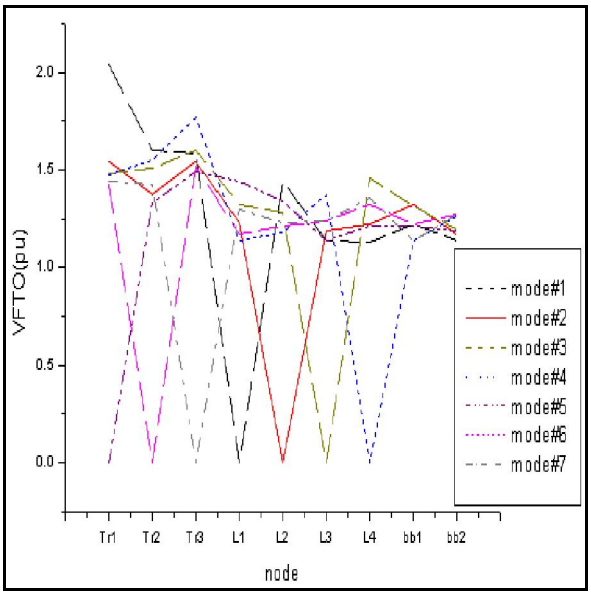

Fig. 4: Comparison between Several Modes of Disconnector Operation

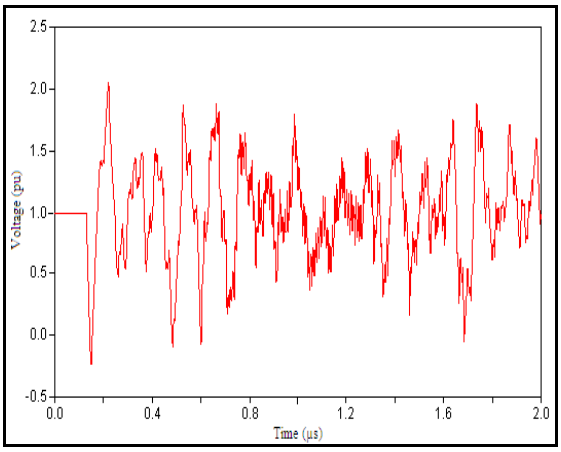

Fig. 5: VFTO at Tr1 (Worst Case)

4.1 The Appropriate Load Side Terminals

The peak magnitude and frequency content of VFT depends on the terminal component connected to the GIS. The terminal components can be cables, gas-insulated lines (GIL), or overhead transmission lines (OHTL). Table 3 gives the electric parameters of these terminal components.

Table 3: Terminal component data

Terminal component	Surge impedance (	Propagation velocity, *v*, (m/µs)
GIL	70	270
OHTL	250	300
XLPE Cable	30	165

The attenuation of VFT with time depends on the type and length of load side terminal component connected to the GIS [8]. Therefore, the VFT can be mitigated by replacement with the appropriate terminals. Simplicity, low cost implementation, and minimum changes in the installed GIS are the main advantages of this technique. Practically in Wadi-Hoff GIS, 5 m OHTL on the source side terminals and 11 m OHTL on the load side terminals are used. Table 4 shows the effect of terminal type on VFTO amplitude. It is clear that the lowest values occur with using cable terminations. Also, the peak values decreased with increasing the cable length. These can be explained as; the cable attenuates the VFTO due to its capacitance to ground, which effectively reduced the VFTO magnitude. Fig. 6 shows the effect of terminal length on VFTO peak at Tr1. It is clearly seen that with length increases the VFTO reduces. Also, Fig. 7 illustrates a comparison between the VFTO at Tr1 in two load terminal cases; 11 m OHTL and 11 m cable.

Table 4: Effect of the Terminal Type on VFTO Amplitude

Terminal Type	VFTO (pu)								
	Tr1	Tr2	Tr3	L1	L2	L3	L4	BB1	BB2
OHTL	2.04	1.60	1.58	0	1.44	1.14	1.13	1.22	1.14
GIL	1.62	1.29	1.35	0	1.37	1.21	1.14	1.23	1.17
Cable	1.26	1.15	1.24	0	1.37	1.13	1.13	1.23	1.19

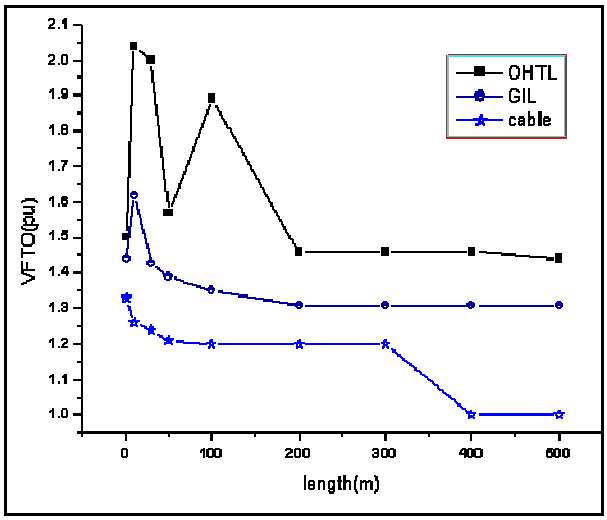

Fig. 6: The peak of the VFTO at Tr1 terminal Vs the load-side terminal length

4.2 The Capacitance at Transformer Terminal

Lumped shunt capacitance is used to damp the VFTO in many applications. The capacitance is arising in surge arrestors, capacitive voltage transformers (CVT), cables, or additional capacitor on the transformer terminals. The capacitance value is changed according to the specifications of the system. Many researches use the capacitance with different values [2,10]. Table 5 gives the effect of the shunt capacitance at the transformer terminals. It is clearly seen that, by increasing the capacitance, the VFTO due to DS re-striking will be further reduced at transformers terminals (Tr1, Tr2, and Tr3). This effect is greatly shown for capacitance values from 0.1 nF to 10 nF, whereas the values above 10 nF do not affect on the results.

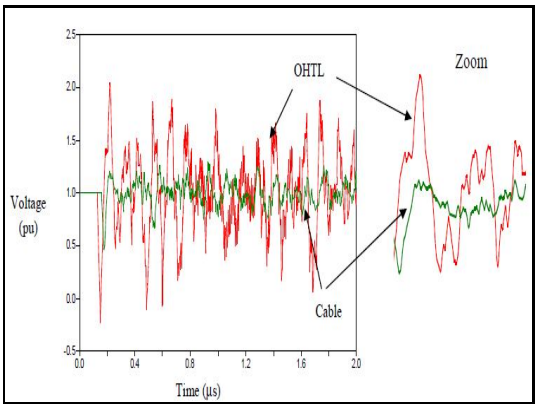

Fig. 7: Comparison between the VFTO at Tr1 in case of OHTL and Cable load terminals

Table 5: Effect of lumped capacitance on VFTO and VFTC

Capacitance (nF)	Tr1		Tr2		Tr3	
	VFTO (pu)	VFTC (pu)	VFTO (pu)	VFTC (pu)	VFTO (pu)	VFTC (pu)
Without	2.04	0.87e-15	1.60	0.21e-31	1.58	0.61e-15
0.1	1.49	0.14e-14	1.21	0.12e-14	1.30	0.13e-14
0.8	1.11	0.30e-14	1.06	0.89e-14	1.06	0.89e-14
1.0	1.08	0.90e-14	1.06	0.91e-14	1.06	0.90e-14
10	1.01	0.72e-13	1	0.67e-13	1.06	0.67e-13
50	1	0.89e-13	1	0.10e-12	1	0.95e-13
100	1	0.62e-12	1	0.62e-12	1	0.62e-12

Fig. 8 shows the influence of the capacitance component on the VFTO and the VFTC at Tr1. Fig. 8 can be used to provide a solution for choosing the optimum value of the capacitance components. This optimum point is achieved at the intersection point of the two curves. So, the adding an extra surge arrester which has a capacitance around 10 nF (the optimum value) can help to achieve the optimum point at Tr1, Tr2, and Tr3.

In order to reduce the VFT at the power transformer, the application of surge capacitors is a feasible alternative due to space limitation and cost, if the suitable capacitance value is selected. Because of impossibility of adding capacitance in high voltage systems, the coupling capacitor voltage transformer with capacitance of 10nF is utilized instead of potential transformer [2].

Fig. 9 illustrates a comparison between the VFTO at Tr1 in case of without and with a capacitance of 10 nF. It is clearly seen the high reduction of oscillations and the value of VFTO.

4.3 Shunt Resistor Disconnector Switching

The switching resistance is connected in parallel with the contacts of the disconnector switch. With the arc to be shunted by the resistance, a part of the arc current flows through the resistance, the arc current will decreases and the rate of deionization of the arc path will be increased [9,10].

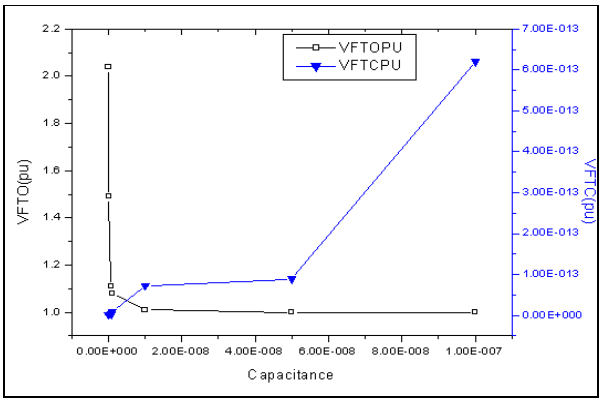

Fig. 8: Influence of Capacitance Component on VFTO and VFTC at Tr1

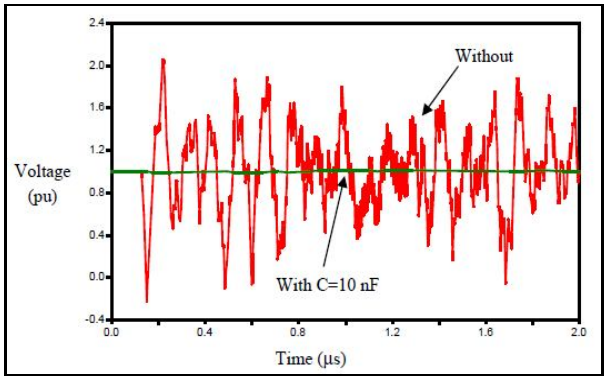

Fig. 9: Comparison between the VFTO at Tr1 in case of without and with shunt capacitance

The installation of opening and closing resistor has a certain application in order to inhibit the generated VFTO in GIS [9]. The shunt resistor acts as a buffering element to the transient process, leaking the remaining charge and absorbing the overvoltage energy. Shunt resistance accelerates the decay of the transient process.

Fig. 10 shows the VFTO when the shunt resistor is used. The effect of changing the resistance value on the VFTO at several points in GIS is used. The amplitude of VFTO is decreased as the switching resistance increases. With increasing the switching resistance from 0 to 400 ohm, the VFTO noticeably decreases. As the switching resistance increased beyond 400 ohm, the VFTO decreased slowly.

It is shown that at the switching resistance of 400 Ω, an optimum solution is get. Fig. 11 shows the comparison between the voltage waveforms of Tr1 in case of with and without shunt resistance.

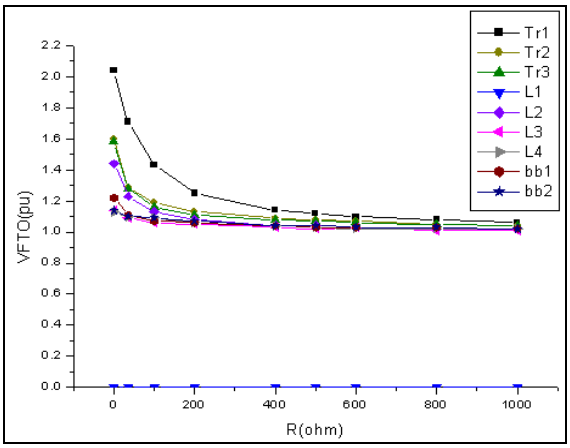

Fig. 10 VFTO at GIS Terminals Vs switching resistor value

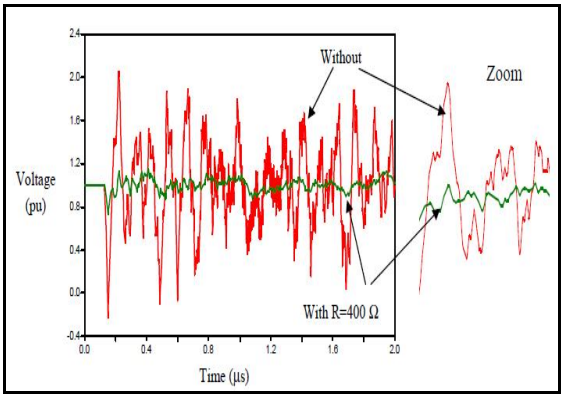

Fig. 11 VFTO at Tr1 with and without shunt resistance

4.4 Ferrite rings Technique

Ferrite is a high-frequency nonlinear magnetic material. The ferrite rings is used around GIS conductors to absorb the transient energy when the DS restrikes to inhibit the VFTO. The ferrite rings can be simplified to a nonlinear inductance and a nonlinear resistance, in series with GIS conductor [7,8].

A ferrite rings of length of 0.47 m with an equivalent diameter of 0.15 m, having an equivalent resistor of 70 Ω and an equivalent inductance of 0.02 mH is used in this study.

Table 6 shows the variation of VFTO at several points due to using many ferrite rings. The results show that the increasing of the number of rings from 1 to 3 gives great effect on reducing the VFTO. More rings gives small effect on the VFTO. So, the optimum result is found with using 3 rings. Fig. 12 illustrates the VFTO when 3 ferrite rings are used at Tr1. It is clearly seen from Table 7 that the reduction of the VFTO is 20% at Tr1, 7% at Tr2, 6% at Tr3, 7% at L2, 2% at L3 and L4, and 2% at BB1 and BB2.

Table 6: Variation of VFTO with the number of ferrite rings

No of rings	VFTO (pu)		
	Tr1	Tr2	Tr3
1	1.45	1.23	1.20
2	1.33	1.17	1.14
3	1.23	1.14	1.12
4	1.20	1.12	1.11
5	1.18	1.11	1.10
6	1.15	1.10	1.09

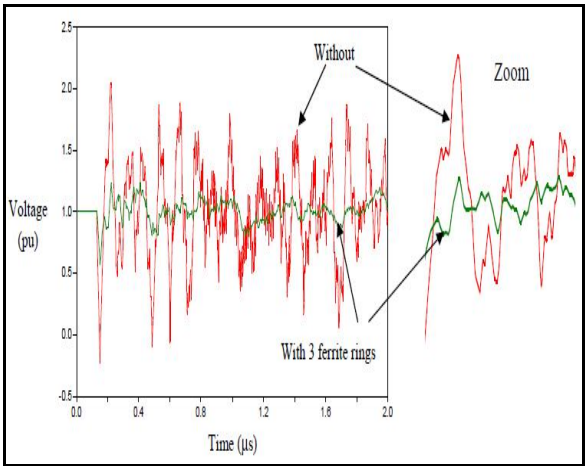

Fig. 12: VFTO at Tr1 with and without ferrite rings

4.5 RC Filter

RC filters (R in parallel with C) have been widely used to protect loads. Also, they have been widely used in vacuum circuit breakers to suppress the over voltages of the arcing [7]. R is used to make energy attenuates and C reduces the circuit oscillation frequency. In this work

RC filter is used as a shunt component next to the main transformer to protect it. R is varied from 50 Ω to 400 Ω and C is changed from 0.01 to 0.2 μF [7]. The optimum mitigation of the VFTO is found at R equal to 50 Ω and at C equal to 0.01 μF.

Table 7 shows the variation of VFTO at several points due to using the RC filter. Also, the percentage reduction in over voltages is given. It is clearly seen that this technique only protects the transformers, whereas the other points in GIS do not affected. Fig. 13 illustrates the comparison between VFTO at Tr1 in case of with and without the RC filter.

Table 7: Variation of VFTO at several points due to using the RC filter

Case	VFTO (pu)					
	Tr1	Tr2	Tr3	L2	L3	BB1
Without shunt RC filter	2.04	1.60	1.58	1.44	1.14	1.22
With shunt RC filter	1.008	1.0071	1.006	1.44	1.14	1.22
% Reduction	50	37	36	0	0	0

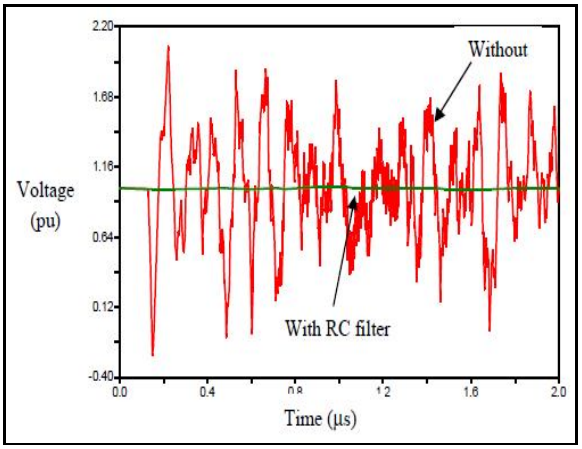

Fig. 13: Comparison between VFTO at Tr1 with and without RC Filter

5. The Proposed Techniques for VFT Mitigation in GIS

Increasing the shunt resistor value gives a reduction of VFTO but this is still associated with high oscillations, as given in section 4.3. Therefore, these oscillations can be fitted by a capacitor or an inductor in series with the resistor. In the following subsections the two techniques are investigated.

5.1 Shunted series RC

When resistance fixed at 400Ω and change capacitance value if increase capacitances above 1μF find no change on VFTO peak and if reduces capacitance below 1μF find great change on reduction of VFTO peak.

Table 8 gives the VFTO at the GIS terminals in case of without and with shunted series RC. Also, the percentage reduction is given. It is found that the reduction is more than that when the shunted resistor is used (as given in Table 6). Fig. 14 shows a comparison between the VFTO at Tr1 in case of with and without shunted series RC, where R is 400 Ω and C is 1pF.

Furthermore, Fig. 15 gives a comparison between the VFTO at Tr1 when a shunted resistor of 400 Ω is used and the proposed shunted series RC with the same resistance and C is 1pF. The figure clearly illustrates the reduction in both the VFTO magnitude and oscillation in case of the proposed technique.

Table 8: VFTO at several points due to using the shunted series RC

Case	VFTO (pu)					
	Tr1	Tr2	Tr3	L2	L3	bb1
Without	2.04	1.60	1.58	1.44	1.14	1.22
With shunted Series R = 400 Ω + C = 1 pF	1.01	1.01	1.01	1.04	1.00	1.00

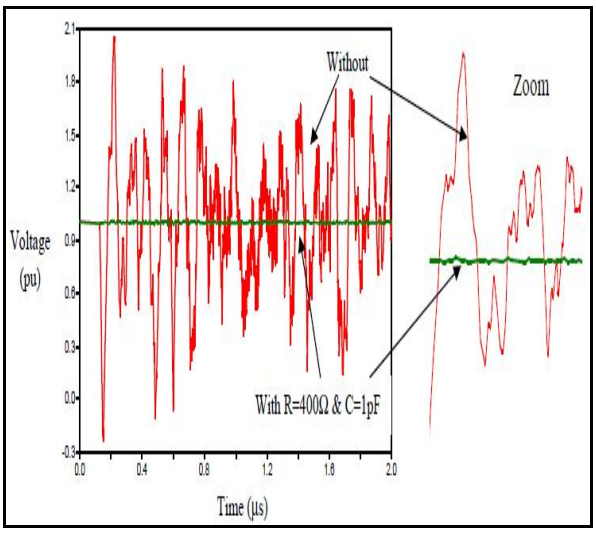

Fig. 14: VFTO at Tr1 with and without shunted series RC

5.2 Shunted series RL disconnector switch

The using of an inductor can limit the dv/dt at transformer terminals. So, shunted series RL is proposed to mitigate the VFTO. The series resistance is chosen as 400 Ω as given in section 4.3 and the series inductance is changed to select the suitable value for this study.

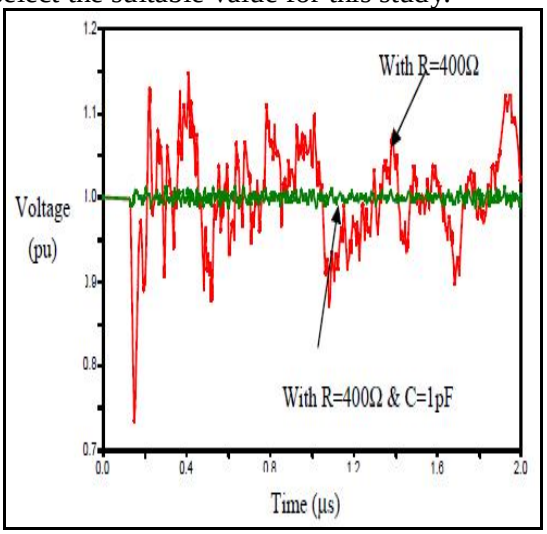

Fig. 15: Comparison between the VFTO when either the shunt resistance or the proposed shunted series RC

Table 9 shows the VFTO when several values of the inductance are applied in series with a 400 Ω resistance. It is found that the VFTO decreases with the inductance increasing. Fig. 16 illustrates a comparison between VFTO in case of without and with the proposed shunted series RL.

Table 9: VFTO due to the proposed shunted series RL, (R=400 Ω)

Inductance in mH	VFTO (pu)					
	Tr1	Tr2	Tr3	L2	L3	bb1
0.01	1.11	1.08	1.08	1.04	1.03	1.02
0.1	1.05	1.04	1.04	1.01	1.01	1.03
1	1	1	1	1	1	1

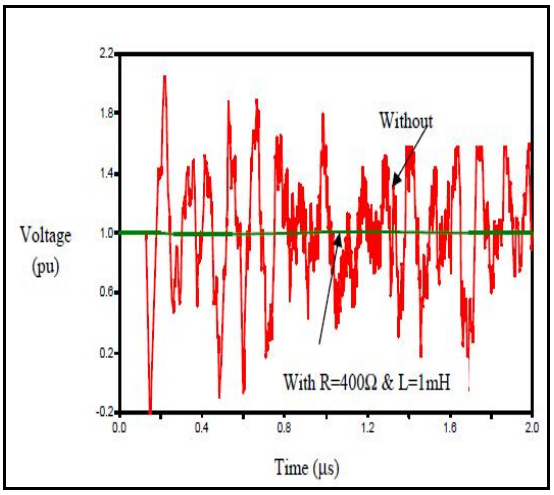

Fig. 16: VFTO at Tr1 with and without shunted series RL

Also, Fig. 17 illustrates a comparison between the VFTO at Tr1 when a shunted resistor of 400 Ω is used and the proposed shunted series RL with the same resistance and L is 0.1mH. The figure clearly shows the reduction in both the VFTO magnitude and oscillation in case of the proposed technique. Furthermore, Fig. 18 gives an overall comparison between the VFTO when only 400 Ω shunted resistor is used and both the proposed techniques; shunted series RC (R=400 Ω and C=1 pF) and shunted series RC (R=400 Ω and L=1 mH). It is clearly seen that the VFTO due to the proposed shunted series RC is less in magnitude and oscillations.

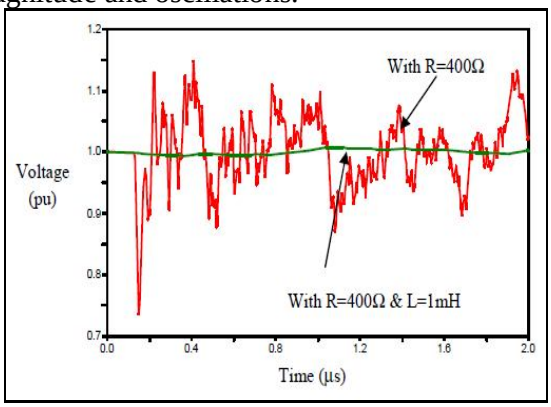

Fig. 17: Comparison between the VFTO when either the shunt resistance or the proposed shunted series RL is used

5.3 Discussion of the Results

Two new techniques are proposed for mitigating VFTO in GIS. One of the proposed techniques uses a capacitor in series with the resistor and the other uses a reactor in series with the resistor. The results of the proposed techniques show that each of them has the ability to reduce the VFTO due to the worst case of the disconnector switching in GIS.

Fig. 18 gives an overall comparison between the VFTO when only 400 Ω shunted resistor is used and both the proposed techniques; shunt series RC (R=400 Ω and C=1 pF) and shunt series RC (R=400 Ω and L=1 mH). It is clearly seen that the VFTO due to the proposed shunt series RL is less in magnitude and oscillations.

The shunt series RC, the shunt series RL, and also the optimum number of the ferrite rings are proposed to be applied at the designers and manufactures stages. Whereas, for the GIS that already in operation the appropriate load side terminals, the capacitance at the transformer terminals, and the RC-filter are considered the economic solutions. In order to overcome the adding of capacitance in high voltage systems, the coupling capacitor voltage transformer is suggested instead of potential transformer

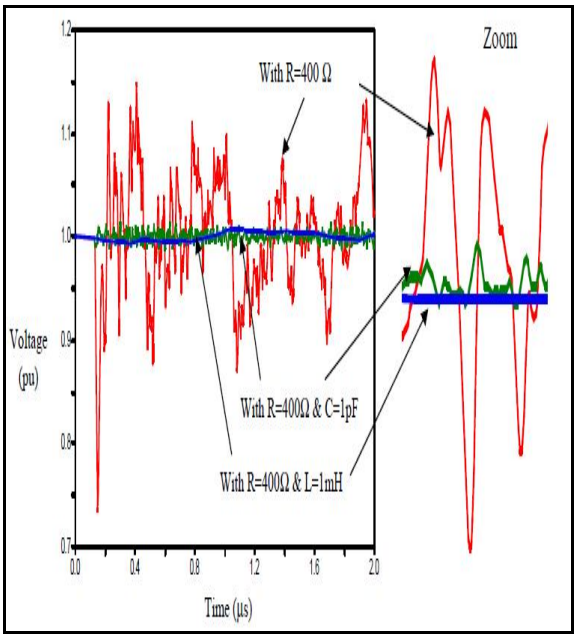

Fig. 18: Comparison between the VFTO due to the shunt resistance, the proposed shunt series RC, and the proposed shunt series RL

6. Conclusion

Disconnector switching in GIS generates VFTO. The mitigation of VFTO is considered a challenge. Many techniques have been used. In this paper new techniques are introduced. The study is implemented on a real 220 kV GIS. The studied GIS is modeled in EMTP/ATP. In this work, many economic techniques are suggested for VFTO mitigation for the real Wadi-Hoff 220 kV GIS. These techniques are the appropriate load side terminals, the capacitance at the transformer terminals, and the RC-filter. These techniques are considered the economic solutions. In order to overcome the adding of capacitance in high voltage systems, the coupling capacitor voltage transformer is suggested instead of potential transformer Furthermore, new techniques are introduced for VFTO mitigation at the designers and manufactures stages. They are the shunt series RC, the shunt series RL, and the optimum number of the ferrite rings. The results show that all these techniques have the ability to reduce the magnitude of the VFTO to an acceptable level. Furthermore, it is found that the shunt series RL also damp the VFTO oscillations.

Reference

[1] A. J. Martinez, "Statistics Assessment of Very Fast Transient Overvoltages in Gas Insulated Substations", IEEE Power Engineering Society Summer Meeting 2000; 2: 882–883.

[2] X. Dong, S. Rosado, Y. Liu, N. C. Wang, E. L. Line and T. Y. Guo, "Study of Abnormal Electrical Phenomena Effects on GSU Transformers", IEEE Transactions on Power Delivery July 2003; 18(3): 835.

[3] V. Vinod Kumar, M. Joy Thomas, and M. S. Naidu," Influence of Switching Conditions on the VFTO Magnitudes in a GIS", IEEE Transaction on Power Delivary, VOL. 16, NO. 4, 2001.

[4] M. Mohana Rao, M. Joy Thomas, and B. P. Singh," Electromagnetic Field Emission From Gas-to-Air Bushing in a GIS During Switching Operations", IEEE Transactions on Eelectromagnetic Compatipility, VOL. 49, NO. 2, 2007.

[5] L. Qingmin and W Minglei, "Simulation Method for the Applications of Ferromagnetic Materials in Suppressing High Frequency Transients Within GIS". IEEE Transactions on Power Delivery July 2007; 22(3): 1628.

[6] Mariusz Stosur, Marcin Szewczyk, Wojciech Piasecki,Marek Florkowski and Marek Fulczyk ," GIS Disconnector Switching Operation– VFTO Study",

Modern Electric Power Systems 2010, MEPS'10 - paper 13.4, Wroclaw, Poland.

[7] J. V. G. Rama Rao, J. Amarnath and S. Kamakshaiah, "Accurate Modeling of Very Fast Transients Overvoltages in A 245kVGIS and Research on Protection Measures", IEEE International conference on Electrical Insulation and Dielectric phenomena((CEIDP2010), West Lafayette, USA..

[8] Wang Zhuo, Wang Weiquan and Wang Qiang, "Research of Suppressing VFTO for 500kV GIS Substation Based on EMTP/ATP", International Conference on E -Business and E -Government (ICEE), 6-8 May 2011.

[9] Wan Yiru, Chen Guang and Zhou Hao," Study on VFTO in UHV GIS Substation" 4th International Conference on Electric Utility Deregulation and Restructuring and Power Technologies (DRPT), 2011.

[10]Ahmad Tavakoli, Ahmad Gholami," Influence of Terminal Components for Suppression of High-Frequency Transients in GIS", International Power and Energy Conference (IPEC 2010), Singapore, 27-29 Oct. 2010.